

A synthetic multicellular system for programmed pattern formation

Supplementary Information

Subhayu Basu, Yoram Gerchman, Cynthia H. Collins, Frances H. Arnold, and Ron Weiss

Plasmid details

Plasmid Name	Genbank Name	Genbank Accession Number	Description
pHD1	pHTSUB-105	T.B.D.	<i>ori</i> ColE1 Cm^R ; $P_{lux(L)}$ -LuxR-G2F, $P_{lux(R)}$ -LacI _{M1} , P_{lac} -GFP(LVA)
pHD2	pHTSUB-104	T.B.D.	<i>ori</i> ColE1 Cm^R ; $P_{lux(L)}$ -LuxR, $P_{lux(R)}$ -LacI _{M1} , P_{lac} -GFP(LVA)
pHD3	pHTSUB-106	bankit680207	<i>ori</i> ColE1 _{mut} Cm^R ; $P_{lux(L)}$ -LuxR, $P_{lux(R)}$ -LacI _{M1} , P_{lac} -GFP(LVA)
pHD2-Red	pHTSUB-105-R	T.B.D.	<i>ori</i> ColE1 Cm^R ; $P_{lux(L)}$ -LuxR, $P_{lux(R)}$ -LacI _{M1} , P_{lac} -DsRed-Express
pLD	pLTSUB-302	T.B.D.	<i>ori</i> p15A Kan^R ; $P_{lux(R)}$ -CI(LVA), $\lambda_{P(R-O12)}$ -LacI
pSND	pLuxI-Tet8	bankit694680	<i>ori</i> ColE1 Cm^R ; $P_{LtetO-1}$ -LuxI
pCFP	pINV-110	T.B.D.	<i>ori</i> p15A Kan^R ; P_{lacIQ} -LacI, P_{lac} -ECFP
pRFP	pFNK-101	T.B.D.	<i>ori</i> p15A Kan^R ; P_{lacIQ} -LacI, P_{lac} -HcRed

Table S1: The high-detect, low-detect, sender, and marker plasmids used in this study.

The effects of repression efficiencies on band-detect gain

We sought to gain a better understanding of how different parameters affect the characteristics of the band detect network. Figure S1 is a contour map showing the effects of CI and LacI repression efficiencies (β_C and β_L) on band-detect *gain*. The contour map was computed from simulations of 25 different values of β_C together with 40 different values of β_L , while keeping all other rate constants the same as those listed in Methods. For a given band-detect AHL response, gain is defined as $\frac{\max_{BD} - \min_{BD}}{\min_{BD}}$, where \max_{BD} is the maximum GFP response over all ranges of AHL considered and $\min_{BD} = \max(\min_{left}, \min_{right})$. The gain computation considers both the minimum GFP response left of the peak (\min_{left}) and the minimum GFP response right of the peak (\min_{right}), and hence a response curve without a clear intermediate band will not obtain a high gain value. The minimum allowed GFP concentrations for \min_{left} and \min_{right} was set to $0.1\mu M$ to avoid unnaturally high gains, while \max_{BD} values below this threshold were considered undetectable and gain was not computed for them. As can be seen, only a particular range of β_C and β_L values results in optimized band-detect responses.

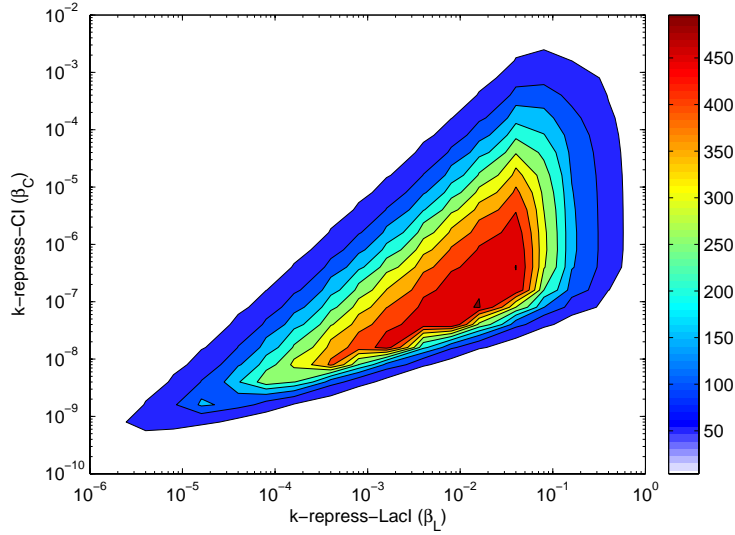
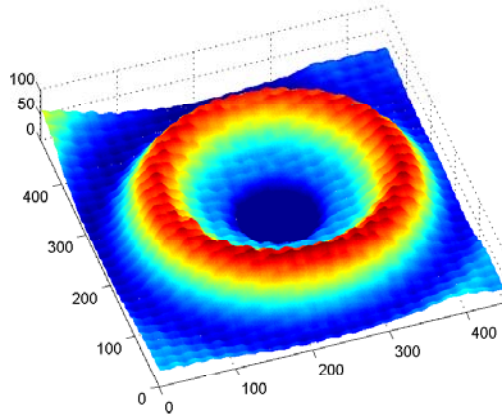
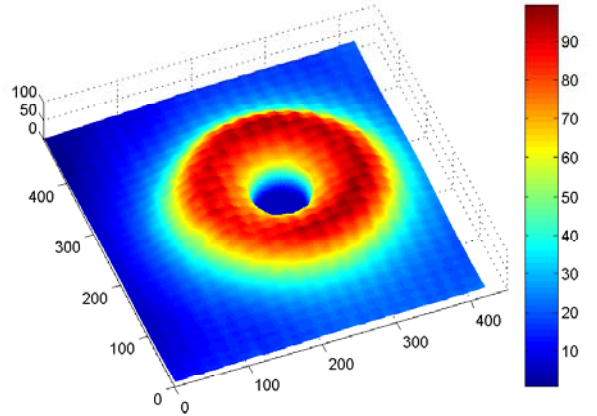


Figure S1: Phase space diagram of band-detect *gain* as a function of the repression efficiencies of LacI (β_L) and CI (β_C).

Surface maps of fluorescence intensities on solid-phase



(a) BD2-Red fluorescence



(b) BD3 fluorescence

Figure S2: Surface maps depicting the fluorescence intensities of BD2-Red and BD3 cells from Figure 3b in the main paper, illustrating the position and width of the distinct rings. Distance in *mm* (X and Y axes). Fluorescence intensities of DsRed-Express (BD2-Red) and GFP (BD3) scaled to a maximum of 100 in arbitrary units (Z axis).